Cellular/Molecular

$P2Y_4$-Mediated Regulation of Na^+ Absorption in the Reissner's Membrane of the Cochlea

Chang-Hee Kim, Hye-Young Kim, Ho Sun Lee, Sun O. Chang, Seung-Ha Oh, and Jun Ho Lee

Department of Otorhinolaryngology, Seoul National University College of Medicine, Sensory Organ Research Institute, Seoul National University Medical Research Center, Chongro-gu, Seoul 110-744, Korea

The epithelial cells of Reissner's membrane (RM) are capable of transporting Na^+ out of endolymph via epithelial Na^+ channel (ENaC). However, much remains to be known as to mechanism of regulation of Na^+ absorption in RM. We investigated P2Y signaling as a possible regulatory mechanism of ENaC in gerbil RM using voltage-sensitive vibrating probe technique and immunohistochemistry. Results showed that UTP induced partial inhibition of the amiloride-sensitive short-circuit current but did not change short-circuit current when applied in the presence of amiloride. The inhibitory effect of UTP was not completely reversible in minutes. The response to UTP was inhibited by reactive blue-2 and 2′,3′-*O*-(4-benzoylbenzoyl)adenosine 5′-triphosphate but not by suramin or pyridoxalphosphate-6-azophenyl-2′, 4′-disulfonic acid, which indicates this P2Y receptor as the $P2Y_4$ subtype. The phospholipase C (PLC) inhibitors 1-[6[[(17β)-3-methoxyestra-1,3,5(10)-trien-17-yl]amino]hexyl]-1*H*-pyrrole-2,5-dione and 1-*O*-octadecyl-2-*O*-methyl-rac-glycero-3-phosphocholine markedly inhibited the effect of UTP on ENaC. In contrast, neither modulation of protein kinase C nor application of 2-aminoehoxydiphenyl borate affected $P2Y_4$-mediated inhibition of ENaC. Immunoreactive staining for $P2Y_4$ was observed in the RM, apical membrane of stria vascularis, spiral ligament, and organ of Corti, including outer hair cell, inner hair cell, outer pillar cell, Deiters' cell, and Hensen cell. These results suggest that the physiological role of $P2Y_4$ receptor in RM is likely to regulate Na^+ homeostasis in the endolymph. The acute inhibition of ENaC activity by activation of $P2Y_4$ receptor is possibly mediated by decrease of phosphatidylinositol 4,5-biphosphate in the plasma membrane through PLC activation.

Introduction

The unique ion composition of cochlear endolymph (high-K^+, low-Na^+) is essential for the function of the sensory hair cells. K^+ transport mechanisms in the cochlea have been mainly elucidated (Wangemann, 2002; Zdebik et al., 2009). The process involved in Na^+ transport in the cochlea also has been described recently. Epithelial cells of the Reissner's membrane (RM) (Lee and Marcus, 2003; C. H. Kim et al., 2009b; S. H. Kim et al., 2009) and outer sulcus cells (Marcus and Chiba, 1999; Lee et al., 2001) were reported to contribute to endolymphatic homeostasis by absorbing Na^+.

The RM consists of two cell layers (tight epithelia, which face endolymph, and mesothelia, which face perilymph) that are separated by a basement membrane and a thin layer of intercellular substance. Recently, there are increasing evidences that RM contributes endolymphatic Na^+ homeostasis via apical epithelial Na^+ channel (ENaC). The amiloride-sensitive Na^+ channel-like immunoreactivity was detected in the luminal surface of the epithelial cells of gerbil RM but not of the mesothelial cells (Mizuta et al., 1995), and all three subunits of ENaC were immunolocalized in rat RM (Zhong and Liu, 2004). ENaC mRNA was localized by *in situ* hybridization in the epithelial cells of rat RM (Couloigner et al., 2001). Transcripts for three subunits of ENaC were present in mouse RM and glucocorticoid upregulated transcriptions for Na^+ transport gene expression (S. H. Kim et al., 2009). The electrogenic transepithelial Na^+ transport was demonstrated in freshly dissected gerbil RM using vibrating probe technique (Lee and Marcus, 2003). It was also demonstrated that transepithelial Na^+ current in RM increases during early development (C. H. Kim et al., 2009b). The α-subunit of Na^+, K^+-ATPase was found to be expressed at the basolateral membrane of the epithelial cells of RM (Iwano et al., 1989). Several types of ion channels, including stretch-activated nonselective cationic channel in the epithelial cell membrane of RM, were identified by patch-clamp studies (Yeh et al., 1997, 1998).

It is known that the activity of ENaC is regulated by hormones such as glucocorticoid, aldosterone, and vasopressin (Garty and Palmer, 1997) and local paracrine factors such as ATP (Kunzelmann et al., 2005). Recently, it has been reported in many other epithelia that extracellular ATP decreases ENaC activity through P2Y purinergic signaling by depletion of phosphatidylinositol 4,5-bisphosphate [$PI(4,5)P_2$] in the plasma membrane (Inglis et al., 1999; Cuffe et al., 2000; Thomas et al., 2001; Lehrmann et al., 2002; Leipziger, 2003). Purinergic receptors appear to form the basis of paracrine and autocrine communication systems in the cochlea (Housley, 1998; Lee and Marcus, 2008), whereas the regulatory mechanism of Na^+ transport through purinergic activation in the inner ear has not been identified yet.

Received July 7, 2009; revised Jan. 19, 2010; accepted Jan. 31, 2010.

This work was supported by Korea Research Foundation Grant KRF-2008-313-E00383 funded by the Korean Government.

Correspondence should be addressed to Dr. Jun Ho Lee, Department of Otorhinolaryngology, Seoul National University College of Medicine, Seoul National University Hospital, 28 Yeongon-dong, Chongro-gu, Seoul 110-744, Korea. E-mail: junlee@snu.ac.kr.

DOI:10.1523/JNEUROSCI.3300-09.2010

 0270-6474/10/303762-08$15.00/0

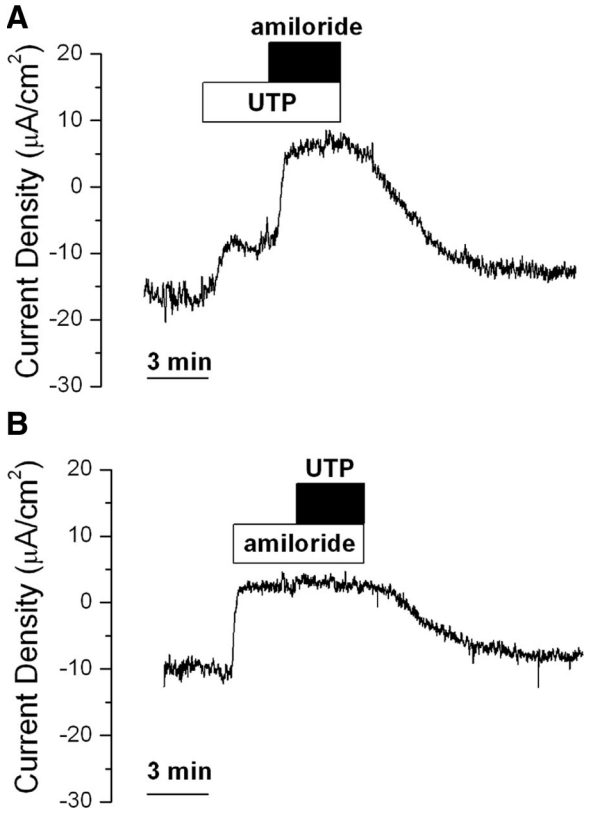

Figure 1. Effect of UTP (100 μM) on I_{sc} in the absence and presence of amiloride (10 μM) in the epithelial cells of the Reissner's membrane. ***A***, Perfusion of UTP inhibited the amiloride-sensitive Na^+ absorption partially. ***B***, Perfusion of amiloride abolished most of baseline I_{sc}. Application of UTP in the presence of amiloride did not change I_{sc}.

Table 1. Effects of UTP (100 μM) on I_{sc} (μA/cm^2) in the absence and presence of amiloride (10 μM)

	Baseline	UTP	Amiloride	Amiloride + UTP
UTP effect in the absence of amiloride ($n = 7$)	-15.0 ± 2.4	-7.9 ± 1.8	NT	1.9 ± 1.1
UTP effect in the presence of amiloride ($n = 6$)	-12.1 ± 2.0	NT[a]	2.8 ± 1.0	2.8 ± 1.0

[a]Not tested.

In this study, we investigated the expression of P2Y receptor and its regulation mechanism of ENaC in the epithelial cells of gerbil RM using vibrating probe technique and immunohistochemistry. Our results demonstrate that $P2Y_4$ receptor is expressed in RM and plays a role in the inhibitory regulation of ENaC activity presumably through depletion of $PI(4,5)P_2$ in the plasma membrane.

Part of this work has been published previously in abstract form (C. H. Kim et al., 2009a).

Materials and Methods

Tissue preparation. Gerbils (3–4 weeks old) were anesthetized with sodium pentobarbital (50–100 mg/kg, i.p.) and killed to remove temporal bones. The methods used for dissecting RM have been described previously (Lee and Marcus, 2003). The stria vascularis was removed from the lateral wall of the apical cochlear turn, and the attached portion of RM was folded over the suprastrial portion of the spiral ligament. The tissue was mounted in a perfusion chamber on the stage of an inverted microscope (Olympus IX70) and continuously perfused at 37°C at an exchange rate of three times per minute. All procedures conformed to protocols approved by the Institutional Animal Care and Use Committee of Seoul National University.

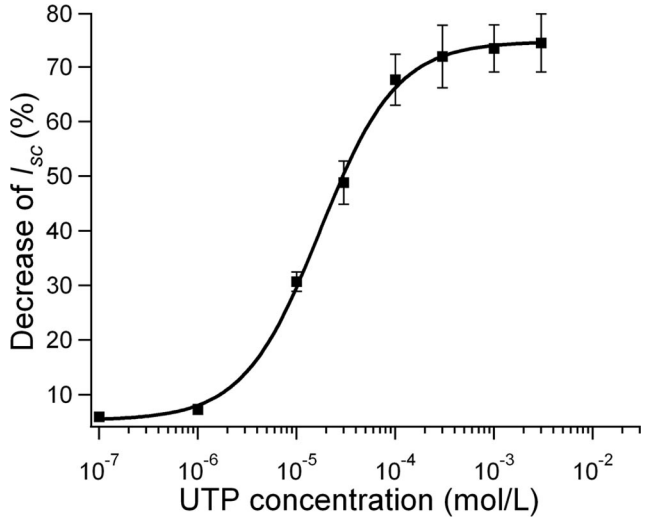

Figure 2. Dose–response relationship of UTP. IC_{50} was 17.2 ± 1.1 μM ($n = 10$ for concentrations of 0.1–300 μM, $n = 5$ for concentrations of 1–3 mM), which was obtained by fitting the data to the Hill equation using IGOR Pro 4.01 (WaveMetrics).

Voltage-sensitive vibrating probe. The vibrating probe technique was used to measure transepithelial currents under short-circuit conditions attributable to the small size of RM epithelium. The diameter of the vibrating probe tip was ~20 μm, and it allowed the detection of voltages in the low nanovolt range; the vibration between two positions within the line of current flow yields voltages that correspond to current flow through the resistive physiological saline (Marcus, 1996). The vibrating probe technique used was identical to a previously described method (Marcus and Shipley, 1994; Marcus, 1996). Briefly, the short-circuit current (I_{sc}) was monitored by vibrating a platinum–iridium wire microelectrode insulated with parylene-C (Micro Electrodes) and that had been coated with platinum-black on its exposed tip. The vibration was ~20 μm along both horizontal (x) and vertical (z) axes. The x-axis was perpendicular to the face of the epithelium, and the probe was positioned at 30 μm from the apical surface of the epithelium using computer-controlled, stepper-motor manipulators (Applicable Electronics) and specialized probe software (ASET version 2.0; Science Wares). The bath references were 26 gauge platinum-black electrodes. Calibration was performed in physiologic saline (see below) using a glass microelectrode (tip <1 μm outer diameter) filled with 3 M KCl as a point source of current. The frequencies of vibration used were in the range 200–400 Hz and were well separated for the two orthogonal directions. Signals from the oscillators driving the probe were also fed to a dual-channel phase-sensitive detector. Asymmetry of probe design yielded different resonant frequencies for the two directions of vibration. X and Z detector signals were connected to a 16 bit analog-to-digital converter (CIO-DAS1602/16; ComputerBoards) in a Pentium IV computer. The sampling interval was 0.6 s, which was the minimum interval allowed by this software. The electrode was positioned where I_{sc} showed a maximum X value and minimum Z value; data are expressed as X value and plotted using Origin software, version 6.1 (OriginLab Software). The output from the vibrating probe depended not only on the specific short-circuit current of the epithelium but also on the position of the probe from the surface of the tissue and on the precise geometry of each tissue sample. The current density reported here refers to the flux at the probe position and represents only a fraction of the current crossing the epithelium. No changes in the relative position of the probe were observed as a result of swelling or shrinking of tissue during experimental treatments.

Immunohistochemistry. Gerbils at the age of 21 d were transcardially perfused with PBS and then with 4% paraformaldehyde in PBS. The cochleas were dissected out and postfixed, by immersion, with a fresh

solution of 4% formaldehyde in PBS for 1 h. After postfixation, the tissues were washed with PBS and transferred to decalcifying solution (0.12 M EDTA, pH 7.2) for 48 h. The EDTA solution was changed after 24 h. The tissues were embedded in Tissue-Tek (Sakura Finetek USA), cryosectioned to a 10 μm thickness using a cryostat (−23°C chamber), and mounted on ProbeOn Plus charged glass slides. The tissue sections were warmed for 15 min at 37°C and then rehydrated with PBS for 10 min. The tissues were then permeabilized, and the nonspecific antigenic sites were blocked using the blocking solution (0.3% Triton X-100 and 10% normal donkey serum in PBS). The sections were incubated overnight at 4°C with the primary antibody. The primary antibody was rabbit anti-$P2Y_4$ (Alomone Labs) diluted at 1:200. The specificity of immunohistochemical stain was controlled by preincubation of antiserum with peptide antigen (the ratio of concentration of peptide to antibody was 1:1) and omitting the primary antibody. The sections were extensively washed with PBS and then incubated in the dark for 1 h at room temperature with the secondary antibody (anti-rabbit Alexa Fluor 488; Invitrogen) diluted in 0.01% Triton X-100 and 1% normal donkey serum in PBS to a final dilution of 1:1000. Finally, the sections were extensively washed with PBS and overlaid with 20 ml of Gel/Mount and a cover glass. The sections were observed with a confocal microscope (LSM510 META; Carl Zeiss).

Solutions and chemicals. The perfusate used as control solution was a perilymph-like physiologic saline of pH 7.4 containing the following (in mM): 150 NaCl, 3.6 KCl, 1 $MgCl_2$, 0.7 $CaCl_2$, 5 glucose, and 10 HEPES. Reactive blue-2 (RB-2) (R-115; Sigma), 2′,3′-*O*-(4-benzoylbenzoyl)adenosine 5′-triphosphate (BzATP) (B-6396; Sigma), suramin (S-2671; Sigma), UTP (U-4630; Sigma), and pyridoxalphosphate-6-azophenyl-2′,4′-disulfonic acid (PPADS) (P-178; Sigma) were directly dissolved in the control solution just before use. Amiloride (A-7410; Sigma), U-73122 (1-[6[[(17β)-3-methoxyestra-1,3,5(10)-trien-17-yl]amino]hexyl]-1*H*-pyrrole-2,5-dione) (U-6756; Sigma), U-73343 (1-[6-((17β-3-methoxyestra-1,3,5(10)-trien-17-yl)amino) hexyl]-2,5-pyrrolidine-dione) (U-6881; Sigma), 1-*O*-octadecyl-2-*O*-methyl-rac-glycero-3-phosphocholine (edelfosine; O-9262; Sigma), GF 109203X (2-[1-(3-dimethylaminopropyl)-1*H*-indol-3-yl]-3-(1*H*-indol-3-yl) maleimide) (catalog #0741; Tocris Bioscience), phorbol myristate acetate (PMA) (P8139; Sigma), and 2-aminoehoxydiphenyl borate (2-APB) (catalog #1224; Tocris Bioscience) were predissolved in dimethylsulfoxide (DMSO) and then diluted to 0.1% DMSO in the control solution before application. DMSO at this concentration had no effect on I_{sc}.

Data presentation and statistics. The baseline I_{sc} values in the control solution were obtained by averaging the data for 9 s just before solution change. Each drug was applied for 2–3 min to see the effect on I_{sc}. For the analysis of the effect of each drug, the data were averaged for 9 s after reaching steady state. Increases or decreases in I_{sc} were considered significant at the $p < 0.05$ level. Statistical comparisons between two means were obtained with *t* test (Mann–Whitney test, if $n < 5$) or paired *t* test (Wilcoxon's signed rank test, if $n < 5$). The data shown were expressed as mean values ± SEM (n = number of tissues) of the I_{sc}.

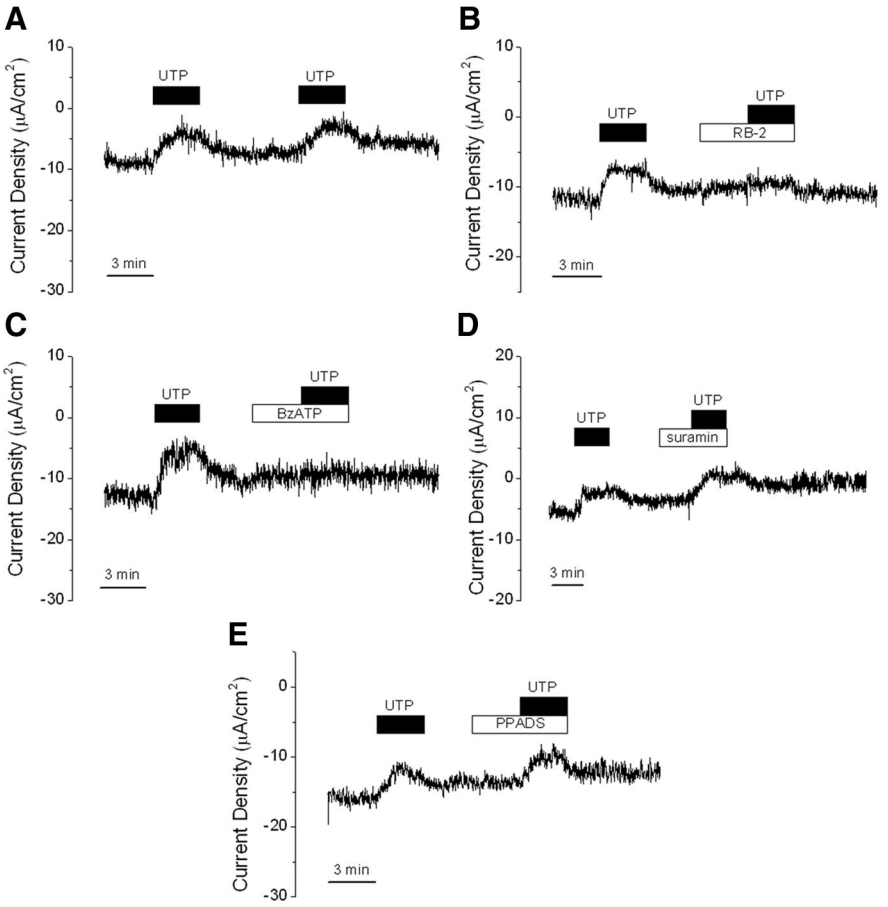

Figure 3. Functional characterization of UTP-responsive P2Y subtype. ***A***, Control experiment (time-controlled) using a protocol that consisted of two consecutive applications of UTP (100 μM) with 6 min interval. I_{sc} decreased in response to perfusion of UTP, and after washout the recovery of I_{sc} was incomplete. The magnitude of inhibition of I_{sc} by the second application of UTP was partially reduced compared with that by the first application of UTP (see Results). ***B–E***, UTP response was blocked by 100 μM RB-2 and 100 μM BzATP but not by 100 μM suramin and 100 μM PPADS.

Results

Effect of UTP on Na^+ absorption in the epithelial cells of RM

We measured baseline I_{sc} of RM in the control solution and the change of I_{sc} after application of amiloride (10 μM) or UTP (100 μM). Negative baseline I_{sc} values were observed in the control solution before application of UTP or amiloride (Fig. 1, Table 1). The application of UTP led to a partial inhibition of I_{sc} (42.9 ± 2.6%, n = 7), and subsequent addition of amiloride inhibited the remaining I_{sc} completely (Fig. 1*A*, Table 1). Interestingly, application of amiloride showed positive I_{sc} values (Fig. 1, Table 1), which was also observed in previous work (Lee and Marcus, 2003), although the cause remains unknown. In contrast, the application of UTP after pretreatment of amiloride, which abolished most of baseline I_{sc}, showed no change of I_{sc} (Fig. 1*B*, Table 1). These results indicate that UTP inhibits amiloride-sensitive Na^+ absorption partially in the epithelial cells of RM.

Dose–response relationship of UTP

UTP inhibited amiloride-sensitive Na^+ absorption in a concentration-dependent manner (from 0.1 μM to 3 mM). The initial I_{sc} was −16.97 ± 0.79 $\mu A/cm^2$ (n = 10), which was reduced by applying UTP to −16.33 ± 0.71 (n = 10, 0.1 μM), −14.93 ± 0.67 (n = 10, 1 μM), −12.03 ± 0.69 (n = 10, 10 μM), −9.31 ± 0.75 (n = 10, 30 μM), −7.55 ± 0.96 (n = 10, 100 μM), −5.94 ± 0.89 (n = 10, 300 μM), −4.45 ± 0.40 (n = 5, 1 mM), and −4.32 ± 0.39 (n = 5, 3 mM). The data were fitted to the following Hill equation (Fig. 2):

$$y = \frac{V_{max}}{1+([UTP]/IC_{50})^h},$$

Table 2. Effects of UTP (100 μM) on I_{sc} (μA/cm^2) in the absence and presence of purinergic antagonists (see Fig. 3)

	Control[a] ($n = 6$)	RB-2, 100 μM ($n = 4$)	BzATP, 100 μM ($n = 4$)	Suramin, 100 μM ($n = 7$)	PPADS, 100 μM ($n = 6$)
Baseline	−11.5 ± 1.0	−9.5 ± 2.1	−15.5 ± 1.6	−9.6 ± 2.3	−11.0 ± 2.5
First UTP	−5.7 ± 0.8	−5.0 ± 1.8	−7.5 ± 1.5	−4.4 ± 2.2	−5.2 ± 2.7
UTP washout	−9.6 ± 0.9	−8.5 ± 1.7	−13.9 ± 1.8	−7.5 ± 2.1	−8.0 ± 2.7
Antagonist	NT[b]	−8.3 ± 1.7	−13.5 ± 1.7	−7.4 ± 2.1	−8.2 ± 2.7
Second UTP	−4.9 ± 0.9	−8.2 ± 1.7	−12.8 ± 2.0	−2.9 ± 2.2	−3.7 ± 2.4
Reduction in the effect of second UTP compared with first UTP (%)	18.4 ± 6.0[c]	97.3 ± 1.6[d,e]	90.2 ± 3.5[d,e]	11.3 ± 10.9[d]	20.4 ± 16.0[d]

[a] This experiment used a protocol that consisted of two consecutive applications of UTP (100 μM) with 6 min interval.

[b] Not tested.

[c] 100 − [(second UTP − UTP washout)/(first UTP − baseline)] × 100.

[d] 100 − [(second UTP − antagonist)/(first UTP − baseline)] × 100.

[e] $p < 0.05$. This value was significantly different from the value observed in the control experiments (18.4%).

Table 3. Effects of UTP (100 μM) on I_{sc} (μA/cm^2) in the absence and presence of P2Y signaling modulators (see Fig. 5)

	U-73122, 10 μM ($n = 8$)	U-73343, 10 μM ($n = 4$)	Edelfosine, 10 μM ($n = 5$)	GF 109203X, 10 μM ($n = 4$)	PMA, 20 nM ($n = 3$)	2-APB, 100 μM ($n = 6$)
Baseline	−13.0 ± 1.5	−12.6 ± 2.3	−17.4 ± 0.9	−12.0 ± 1.8	−11.2 ± 2.8	−12.0 ± 1.2
First UTP	−7.2 ± 1.4	−7.6 ± 1.7	−8.7 ± 0.8	−7.1 ± 1.7	−5.9 ± 1.8	−6.2 ± 1.3
UTP washout	−10.9 ± 1.4	−10.5 ± 1.9	−14.4 ± 0.8	−10.4 ± 1.8	−9.1 ± 2.3	−10.1 ± 1.2
Antagonist	−12.0 ± 1.4	−10.5 ± 2.0	−14.0 ± 0.7	−10.3 ± 1.8	−9.1 ± 2.4	−10.4 ± 1.3
Second UTP	−11.9 ± 1.4	−6.8 ± 2.3	−13.9 ± 0.8	−6.3 ± 1.5	−5.3 ± 2.6	−6.1 ± 1.4
Reduction in the effect of second UTP compared with first UTP (%)[a]	97.6 ± 0.7[b]	19.0 ± 18.7	98.4 ± 1.6[b]	17.7 ± 9.4	22.7 ± 10.6	26.4 ± 2.8

[a] 100 − [(second UTP − antagonist)/(first UTP − baseline)] × 100.

[b] $p < 0.05$. Statistical significance was compared with the value (18.4%) observed in the control experiments in Table 2.

where y is the predicted inhibition by UTP, V_{max} is a maximum inhibition, [UTP] is UTP concentration, IC_{50} is the UTP concentration of the half-maximal inhibitory effect, and h is the Hill coefficient (slope factor) of sigmoidicity. Best-fit estimates yielded maximum inhibition 74.7 ± 0.9%, IC_{50} of 17.2 ± 1.1 μM, and Hill coefficient of 1.1 ± 0.1.

Characterization of UTP-responsive P2Y receptor

We introduced the antagonists of purinergic receptors to characterize the subtype of UTP-responsive P2Y receptor and compared the effects of UTP on Na^+ absorption in the absence and presence of each antagonist (Fig. 3, Table 2). We have consistently observed that the effect of UTP on Na^+ absorption was not completely reversible in minutes. The recovery rate of I_{sc} was 75.5 ± 2.4% at 3 min after UTP washout ($n = 56$) (Tables 2, 3). Therefore, we conducted control experiments (time-controlled) using the protocol consisting of two consecutive applications of UTP (100 μM) with 6 min interval (Fig. 3*A*). The magnitude of inhibition of I_{sc} by the second application of UTP was partially reduced (18.4 ± 6.0%, $n = 6$) compared with that by the first application of UTP in the control experiments (Fig. 3*A*, Table 2). This ratio of the magnitude of inhibition obtained in the control experiments was statistically compared with that obtained in the each experimental protocol using antagonists of purinergic receptors (Fig. 3*B–E*) and phospholipase C (PLC) signaling modulators (Fig. 4) to determine the effect of each drug on Na^+ absorption.

The application of RB-2 (100 μM) for 3 min resulted in no significant change in I_{sc} ($n = 4$) (Fig. 3*B*, Table 2). The magnitude of inhibition of I_{sc} by UTP in the presence of RB-2 was reduced by 97.3 ± 1.6% ($n = 4$) (Fig. 3*B*, Table 2) compared with that observed in the absence of RB-2. This value (97.3% reduction) was significantly different from the value (18.4% reduction) observed in the control experiments. UTP response was significantly reduced by the application of 100 μM BzATP ($n = 4$, 90.2% reduction) (Fig. 3*C*). In contrast, neither 100 μM suramin (Fig. 3*D*) nor 100 μM PPADS (Fig. 3*E*) had any significant effect on the action of UTP. The magnitude of inhibition of I_{sc} by UTP in the presence of suramin or PPADS was reduced by 11.3 ± 10.9% ($n = 7$) (Fig. 3*C*, Table 2) or 20.4 ± 16.0% ($n = 6$) (Fig. 3*D*, Table 2) compared with that observed in the absence of each antagonist. These values were not significantly different from the data (18.4% reduction) observed in the control experiments. These pharmacological results indicate that UTP-responsive P2Y receptor is $P2Y_4$ subtype (see Discussion).

Mechanism of $P2Y_4$-mediated regulation of ENaC

We investigated the role of PLC signaling cascade in the regulation of ENaC activity by UTP. We perfused 100 μM UTP for 3 min. After washout of UTP for 3 min, drugs (U-73122, U-73343, GF 109203X, PMA, and 2-APB) were applied for 6 min. UTP was added during the last 3 min of perfusion of drugs. Perfusion of U-73122 (10 μM) had no significant effect on I_{sc}, but the magnitude of inhibition of I_{sc} by UTP in the presence of U-73122 was reduced by 97.6 ± 0.7% ($n = 8$) (Fig. 4*A*, Table 3) compared with that observed in the absence of U-73122. This value was significantly different from the value (18.4% reduction) observed in the control experiments (Table 2). UTP response was significantly reduced by the application of 10 μM edelfosine ($n = 5$, 98.4% reduction) (Fig. 4*C*, Table 3). U-73343, GF 109203X, PMA, and 2-APB showed no effect on I_{sc} and did not affect the effect of UTP on Na^+ absorption (Fig. 4*B*,*D*,*E*,*F*, Table 3). The sensitivities of purinergic antagonists and modulators of P2Y signaling to UTP response were summarized in Figure 5.

Dose–response relationship of RB-2 and U-73122

Dose–response relationship of RB-2 on $P2Y_4$ receptor was obtained while perfusing 100 μM UTP. For the control experiment, 100 μM UTP was applied for 16 min to investigate the change of I_{sc} during the prolonged perfusion of UTP before assessing the dose–response relationship of RB-2. The initial I_{sc} was −17.89 ± 1.20 μA/cm^2 and changed to −9.96 ± 0.19 μA/cm^2 at 2 min after UTP application and to −10.05 ± 0.36 μA/cm^2 at the end of UTP application ($n = 4$) (Fig. 6*A*). There was no significant I_{sc}

change during the prolonged perfusion of UTP after reaching the plateau.

RB-2 inhibited UTP response in a concentration-dependent manner ($n = 4$ at each concentration from 0.1 to 300 μM) (Fig. 6*B*). The initial I_{sc} was -18.34 ± 1.93 $\mu A/cm^2$ and changed to -7.18 ± 0.94 $\mu A/cm^2$ at 2 min after application of 100 μM UTP. Application of RB-2 increased I_{sc} to -7.55 ± 1.10 (0.1 μM), -9.92 ± 0.77 (1 μM), -11.99 ± 0.87 (3 μM), -14.12 ± 0.69 (10 μM), -15.97 ± 1.02 (30 μM), -17.95 ± 1.73 (100 μM), and -17.99 ± 1.74 $\mu A/cm^2$ (300 μM). The data were fitted to the Hill equation (Fig. 6*C*). The estimated IC_{50} value of RB-2 was 4.9 ± 1.0 μM.

The dose–response relationship of U-73122 was obtained in the presence of 100 μM UTP. The control experiments for the dose–response relationship of U-73122 were same to those used in the dose–response relationship of RB-2. U-73122 inhibited UTP response in a concentration-dependent manner ($n = 4$ at each concentration from 0.01 to 30 μM) (Fig. 6*D*). The initial I_{sc} was -19.02 ± 0.27 $\mu A/cm^2$ and changed to -9.47 ± 0.59 $\mu A/cm^2$ at 2 min after application of 100 μM UTP. Application of U-73122 increased I_{sc} to -9.75 ± 0.68 (0.01 μM), -12.06 ± 0.35 (0.1 μM), -13.80 ± 0.31 (0.3 μM), -15.85 ± 0.22 (1 μM), -17.40 ± 0.37 (3 μM), -18.21 ± 0.56 (10 μM), and -18.32 ± 0.61 $\mu A/cm^2$ (30 μM). The data were fitted to the Hill equation (Fig. 6*E*). The IC_{50} value of U-73122 was 3.1 ± 0.2 μM.

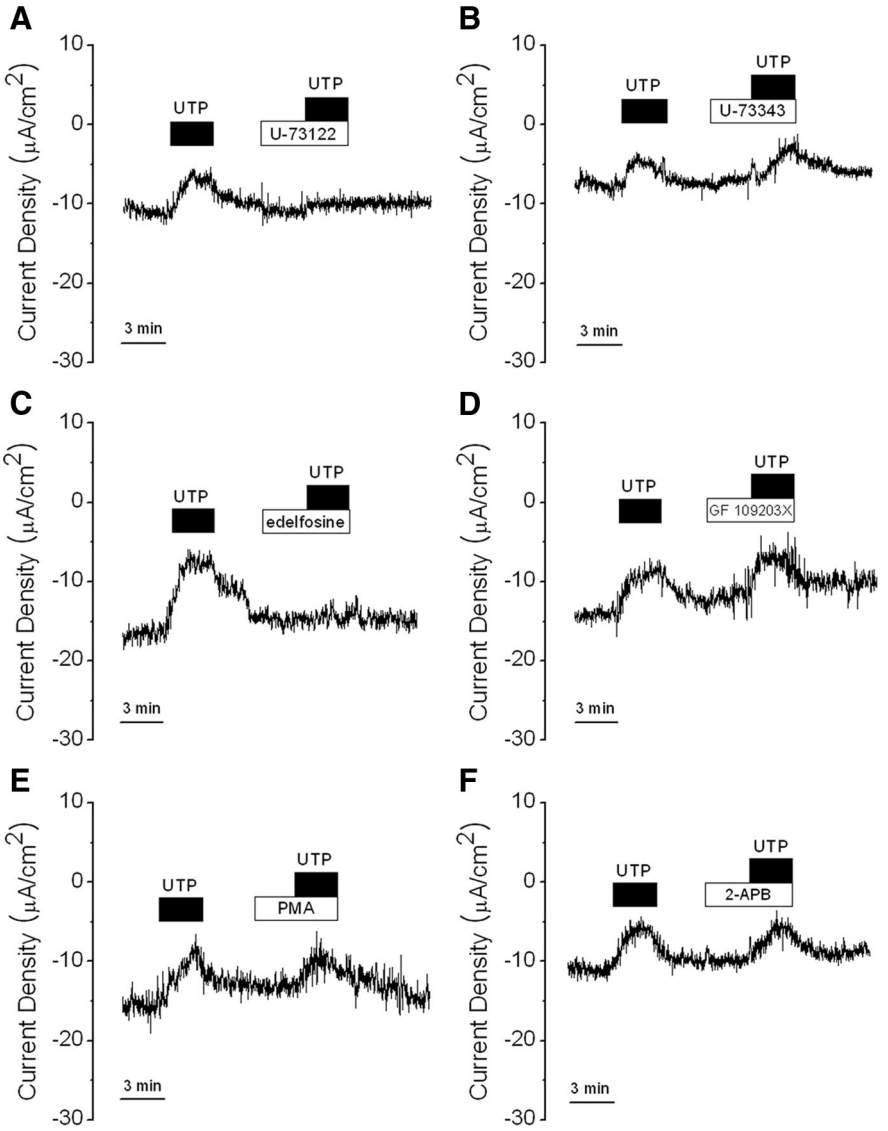

Figure 4. Involvement of P2Y signaling cascade. ***A***, ***B***, UTP (100 μM) response was inhibited by U-73122 (PLC inhibitor, 10 μM) but not by U-73343 (inactive analog of U-73122, 10 μM). ***C***, Edelfosine (10 μM), a PLC inhibitor, significantly inhibited UTP response. ***D–F***, GF 109203X (PKC inhibitor, 10 μM), PMA (PKC activator, 20 nM), and 2-APB (IP_3 receptor blocker, 100 μM) did not affect UTP effect on Na^+ absorption.

Immunohistochemistry of $P2Y_4$ receptor

Immunoreactive staining for $P2Y_4$ was observed in the epithelial cells of RM, apical membrane of the stria vascularis, spiral ligament (Fig. 7*A*,*D*,*E*), and organ of Corti (Fig. 7*A*,*G*,*H*). In the organ of Corti, moderate staining was observed in the outer hair cells, inner hair cells, outer pillar cells, and Hensen's cells. The greatest intensity of staining was observed in Deiters' cells and head of outer pillar cells (Fig. 7*G*,*H*). Anti-$P2Y_4$ antibody preabsorbed with antigenic peptide was negative for staining (Fig. 7*B*), and omitting the primary antibody from the procedure also showed negative results (Fig. 7*C*).

Discussion

Inhibition of Na^+ absorption by activation of $P2Y_4$ receptor

In this study, the presence of metabotropic P2Y receptor, which regulates the activity of amiloride-sensitive Na^+ channel, was demonstrated in the epithelial cells of RM, and pharmacologic study pointed to P2Y subtype as $P2Y_4$ receptor. UTP is not a specific agonist of $P2Y_4$ but an agonist of several subtypes of P2Y receptors, such as rat $P2Y_2$, $P2Y_4$, and $P2Y_6$ (von Kügelgen, 2006). $P2X_2$ purinergic receptors studied by another group (King et al., 1998) would not be activated by the agonist UTP. Suramin and PPADS are also not specific antagonists of P2X and/or P2Y receptor subtype. Suramin is a potent antagonist of rat $P2Y_2$ (Wildman et al., 2003) but not of $P2Y_4$ (Bogdanov et al., 1998; Wildman et al., 2003). PPADS is an antagonist of rat $P2X_1$, $P2X_2$, $P2X_3$, $P2X_5$, $P2X_7$, and $P2Y_1$ (Ralevic and Burnstock, 1998) and of human and mouse $P2Y_6$ (Robaye et al., 1997; Housley et al., 2002). RB-2 is a potent antagonist of rat $P2Y_4$ receptor, which was expressed in *Xenopus oocytes* (Wildman et al., 2003). BzATP is a potent agonist for rat $P2Y_2$ and an antagonist for rat $P2Y_4$ receptor, which was expressed in *Xenopus oocytes* (Wildman et al., 2003). These criteria applied to the present results point to the P2Y purinergic receptor in the epithelial cells of RM as the $P2Y_4$ subtype.

Our results agree with those reported in other epithelial cell types in several aspects. First, the activation of P2Y receptors by 100 μM UTP resulted in partial inhibition of amiloride-sensitive Na^+ transport (42.9%) (Fig. 1*A*). This partial inhibition at this concentration has been reported in other epithelia, i.e., 76% in

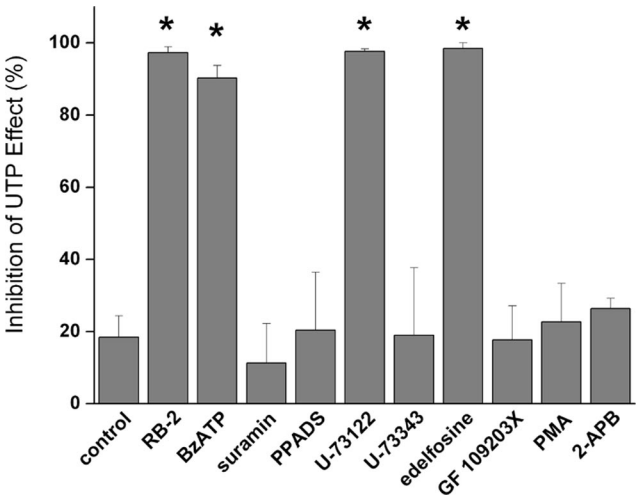

Figure 5. Summary of the effects of purinergic receptor antagonists and modulators of P2Y intracellular signaling on UTP response. The inhibitory effects of UTP on amiloride-sensitive Na^+ absorption were markedly reduced by RB-2, BzATP, U-73122, and edelfosine. $*p < 0.05$.

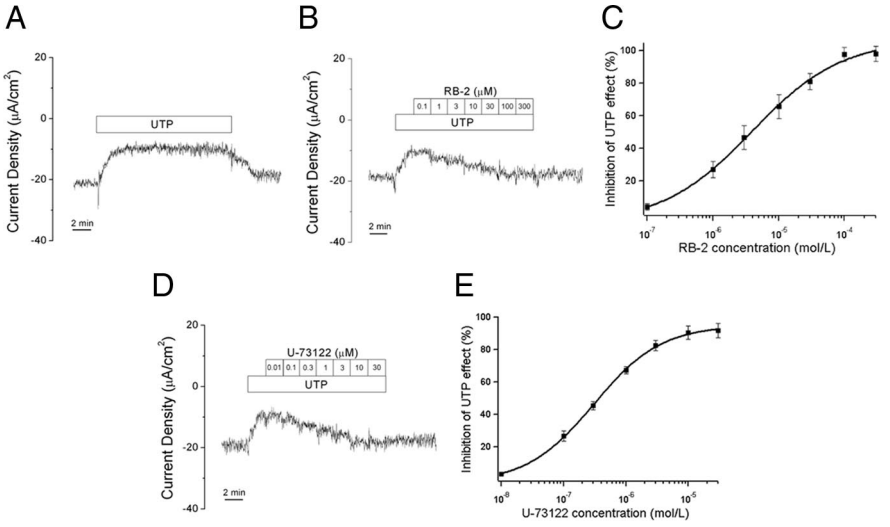

Figure 6. Dose–response relationship of RB-2 and U-73122. ***A***, Control experiment in which 100 μM UTP was applied for 16 min. ***B***, A representative dose–response effect of RB-2 on UTP response. ***C***, Dose–response curve of RB-2. IC_{50} was 4.9 ± 1.0 μM ($n = 4$). ***D***, A representative dose–response effect of U-73122 on UTP response. ***E***, Dose–response curve. IC_{50} was 3.1 ± 0.2 μM ($n = 4$). Datasets were fitted using the Hill equation.

human bronchial epithelia (Devor and Pilewski, 1999), 40% in normal human airways (Inglis et al., 1999), and 49.1% in mouse distal nephron (Lehrmann et al., 2002). Second, the concentration dependence of the inhibitory effect of UTP on amiloride-sensitive Na^+ current had an IC_{50} value of 17.2 ± 1.1 μM (Fig. 2). IC_{50} values for concentration–response of UTP or ATP in other epithelia such as distal colon and cortical collecting duct of kidney were in the range of 0.6–30 μM (Cuffe et al., 2000; Yamamoto and Suzuki, 2002; Matos et al., 2007). Third, the inhibitory effect of UTP was not completely reversible after washout (75.5 ± 2.4% recovered). Although slow perfusion rate may be one of the reasons of the limited reversibility, this phenomenon has also been reported in other studies (Marcus et al., 2005; Matos et al., 2007). ATP- or UTP-induced inhibition of the amiloride-sensitive Na^+ current was not completely reversible in other organs, i.e., ~85 or 89% recovered in mouse cortical collecting duct cells (Cuffe et al., 2000; Lehrmann et al., 2002). Interestingly, it was reported that it took 60 min for complete washout in human cystic fibrosis airways (Mall et al., 2000).

Mechanism of $P2Y_4$-mediated inhibition of amiloride-sensitive Na^+ absorption

Involvement of PLC activation was demonstrated by the markedly reduced effect of UTP in the presence of U-73122, a PLC inhibitor, but not in the presence of U-73343, an inactive analog. Another PLC inhibitor, edelfosine, also significantly inhibited UTP response. Furthermore, we investigated whether protein kinase C (PKC) modulators affect the effect of UTP on amiloride-sensitive Na^+ channel. GF 109203X, a PKC inhibitor, and PMA, a PKC activator, induced no significant effect on UTP response; therefore, it is not likely that PKC signaling branch is involved in the acute regulation of ENaC activity. This finding was consistent with another previous report (Pochynyuk et al., 2008). It has been reported that activation of PLC signaling inhibits ENaC activity either by activating PKC or depletion of the inner membrane $PI(4,5)P_2$ content (Kunzelmann et al., 2005). The activation of PKC is known to evoke later response and to maintain long-term (up to 48 h) downregulation of ENaC by decreasing plasma membrane levels of the channel (Stockand et al., 2000; Booth and Stockand, 2003). The level of γ-ENaC decreased by PKC with a time constant of 3.7 h, and the level of β-ENaC decreased in 13.9 h. The fact that treatment of tissues with 2-APB, a cell-permeable antagonist of inositol trisphosphate (IP_3) receptor and store-operated channels (Bootman et al., 2002), did not affect UTP effect on ENaC activity suggests that the involvement of the second branch of the PLC pathway (IP_3 production) in response to UTP is negligible. It has been shown that 2-APB also inhibits gap junctions composed of connexin 26 or connexin 32 and modifies the transient receptor potential channel activity (Xu et al., 2005; Tao and Harris, 2007). Anionic $PI(4,5)P_2$ is located in the inner layer of plasma membrane and interacts with ion channels or transporters (Hilgemann et al., 2001). Recently, evidences that dynamic interaction between $PI(4,5)P_2$ and β-subunit of ENaC enhances open probability of ENaC and depletion of $PI(4,5)P_2$ in plasma membrane by activation of metabotropic purinergic receptor decreases ENaC activity, have been reported (Kunzelmann et al., 2005; Ma et al., 2007; Pochynyuk et al., 2008). Together, UTP-mediated inhibition of ENaC activity in the epithelial cells of RM might be caused by decreased open probability of ENaC attributable to depletion of $PI(4,5)P_2$ concentration in the plasma membrane.

Immunolocalization of $P2Y_4$ receptors

The electrophysiological evidence of the presence of $P2Y_4$ receptors in RM was further supported by immunohistochemical staining with which $P2Y_4$ receptors were localized in RM. However, subcellular expression pattern could not be discerned within the extremely thin epithelia of RM by immunohistochemistry, and the technique for measuring I_{sc} allowed no means to control the sidedness of agonist application. We could get additional findings as below. In the stria vascularis, as re-

ported previously (Sage and Marcus, 2002), immunoreactivity for $P2Y_4$ receptor was shown at the apical membrane of the strial marginal cells in which $P2Y_4$ is known to inhibit K^+ secretion via KCNQ1/KCNE1 K^+ channel (Marcus et al., 1998; Loussouarn et al., 2003).

Interestingly, $P2Y_4$ receptors were identified in many cellular types of the organ of Corti. The finding that Deiters' cells had the most intense immunostaining for $P2Y_4$ was consistent with the previous report in guinea pigs (Parker et al., 2003). $P2Y_4$ was also localized in the sensory hair cells. The inner hair cells showed moderate immunostaining in the lateral wall of cell body, and the outer hair cells showed heterogeneous distribution of $P2Y_4$ receptors. In outer hair cells, immunoreactivity was detected more intensely at the apex around the cuticular plate that is facing endolymphatic space than at the lateral wall of cell body. This finding was inconsistent with that $P2Y_4$ receptors were expressed only at the basal pole of the isolated outer hair cells in guinea pigs (Szücs et al., 2004). To our knowledge, the functional roles of P2Y receptors in these cells are uncertain yet.

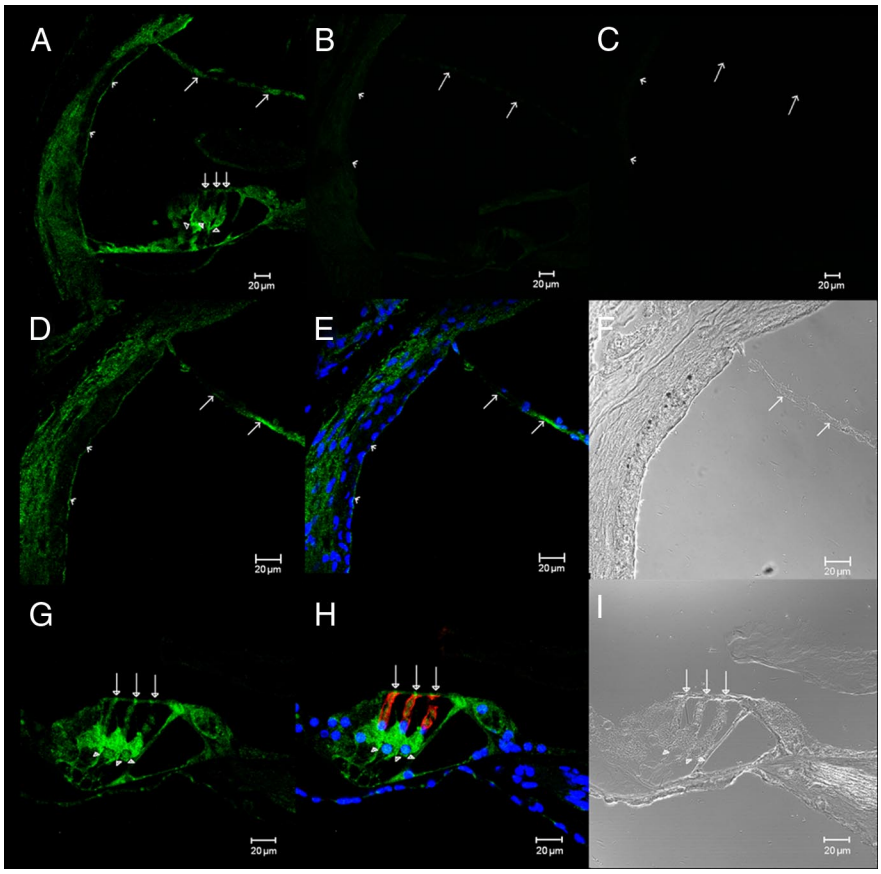

Figure 7. Immunohistochemical localization of $P2Y_4$ receptors in the cochlea (blue, DAPI nuclear stain; green, anti-$P2Y_4$ stain; red, anti-prestin stain). ***A***, Low-power view of cross-section through the cochlear duct (open arrows, Reissner's membrane; open arrowheads, apical membrane of stria vascularis; filled arrows, cuticular plate of outer hair cells; filled arrowheads, Deiters' cells). ***B***, ***C***, Negative controls. Preabsorption of $P2Y_4$ antibody with antigenic peptide (***B***) or the omission of the primary antibody for $P2Y_4$ receptor (***C***) revealed no significant immunoreactivity. ***D*** ($P2Y_4$), ***E*** (merged), ***F*** (bright field), $P2Y_4$ immunoreactivity was observed in the Reissner's membrane (open arrows), the apical membrane of strial marginal cells (open arrowheads), and spiral ligament. ***G*** ($P2Y_4$), ***H*** (merged), ***I*** (bright field), In the organ of Corti, most cellular types showed immunoreactive staining for $P2Y_4$. The most intense immunolabeling was detected in the Deiters' cells (filled arrowheads). In the outer hair cells, immunohistochemical distribution of $P2Y_4$ receptors was heterogeneous; intense staining was observed at the apical part, close to the cuticular plate (filled arrows), whereas lateral wall of cell body was moderately stained. The inner hair cells were moderately stained in the lateral wall of cell body. Intense staining was seen in the head of the outer pillar cells.

Physiological significance of $P2Y_4$ receptors in epithelial cells of RM

ATP is released from most cell types and functions as a natural agonist. UTP has been reported to be released from cultured cells of different tissues and suggested that it may act as a natural agonist (Lazarowski et al., 1997; Homolya et al., 2000). In the cochlea, it has been considered that nucleotide such as ATP reduces the sensitivity of sound transduction, especially under the condition of noise exposure (Munoz et al., 2001; Housley et al., 2002). When noise exposure elevates ATP levels in the scala media, there may be the increase of parasensory K^+ extrusion from endolymph via ionotropic P2X receptor bounding the endolymphatic duct (Housley et al., 1998) and also the decrease of K^+ transport into scala media from the stria vascularis by activation of metabotropic $P2Y_4$ receptor (Marcus and Scofield, 2001). In view of Na^+, $P2Y_4$ receptor that is expressed in RM mediates to inhibit Na^+ absorption from the endolymph, and consequently Na^+ concentration in the scala media can increase. However, because the natural agonist ATP and, possibly UTP, can act on purinergic receptors widely distributed in the epithelial cells of the endolymphatic duct, the total net movement of endolymphatic Na^+ would be regulated by balance of P2X and P2Y purinergic signaling.

In conclusion, $P2Y_4$ receptor was expressed in the epithelial cells of RM. It is likely that the physiological role of $P2Y_4$ receptor is to regulate Na^+ extrusion from the endolymph to the perilymph, probably in response to noise exposure. The acute inhibition of ENaC activity by activation of $P2Y_4$ receptor is possibly mediated by decrease of $PI(4,5)P_2$ in the plasma membrane through PLC activation.

References

Bogdanov YD, Wildman SS, Clements MP, King BF, Burnstock G (1998) Molecular cloning and characterization of rat P2Y4 nucleotide receptor. Br J Pharmacol 124:428–430.

Booth RE, Stockand JD (2003) Targeted degradation of ENaC in response to PKC activation of the ERK1/2 cascade. Am J Physiol Renal Physiol 284:F938–F947.

Bootman MD, Collins TJ, Mackenzie L, Roderick HL, Berridge MJ, Peppiatt CM (2002) 2-aminoethoxydiphenyl borate (2-APB) is a reliable blocker of store-operated Ca^{2+} entry but an inconsistent inhibitor of InsP3-induced Ca^{2+} release. FASEB J 16:1145–1150.

Couloigner V, Fay M, Djelidi S, Farman N, Escoubet B, Runembert I, Sterkers O, Friedlander G, Ferrary E (2001) Location and function of the epithelial Na channel in the cochlea. Am J Physiol Renal Physiol 280:F214–F222.

Cuffe JE, Bielfeld-Ackermann A, Thomas J, Leipziger J, Korbmacher C (2000) ATP stimulates Cl^- secretion and reduces amiloride-sensitive Na^+ absorption in M-1 mouse cortical collecting duct cells. J Physiol 524:77–90.

Devor DC, Pilewski JM (1999) UTP inhibits Na^+ absorption in wild-type and DeltaF508 CFTR-expressing human bronchial epithelia. Am J Physiol 276:C827–C837.

Garty H, Palmer LG (1997) Epithelial sodium channels: function, structure, and regulation. Physiol Rev 77:359–396.

Hilgemann DW, Feng S, Nasuhoglu C (2001) The complex and intriguing lives of PIP2 with ion channels and transporters. Sci STKE 2001:re19.

Homolya L, Steinberg TH, Boucher RC (2000) Cell to cell communication in response to mechanical stress via bilateral release of ATP and UTP in polarized epithelia. J Cell Biol 150:1349–1360.

Housley GD (1998) Extracellular nucleotide signaling in the inner ear. Mol Neurobiol 16:21–48.

Housley GD, Luo L, Ryan AF (1998) Localization of mRNA encoding the P2X2 receptor subunit of the adenosine 5′-triphosphate-gated ion channel in the adult and developing rat inner ear by in situ hybridization. J Comp Neurol 393:403–414.

Housley GD, Jagger DJ, Greenwood D, Raybould NP, Salih SG, Järlebark LE, Vlajkovic SM, Kanjhan R, Nikolic P, Muñoz DJ, Thorne PR (2002) Purinergic regulation of sound transduction and auditory neurotransmission. Audiol Neurootol 7:55–61.

Inglis SK, Collett A, McAlroy HL, Wilson SM, Olver RE (1999) Effect of luminal nucleotides on Cl^- secretion and Na^+ absorption in distal bronchi. Pflugers Arch 438:621–627.

Iwano T, Yamamoto A, Omori K, Akayama M, Kumazawa T, Tashiro Y (1989) Quantitative immunocytochemical localization of Na^+,K^+-ATPase alpha-subunit in the lateral wall of rat cochlear duct. J Histochem Cytochem 37:353–363.

Kim CH, Kim HY, Chang SO, Oh SH, Lee JH (2009a) P2Y4 receptor-mediated regulation of amiloride-sensitive sodium transport in the Reissner's membrane of gerbil cochlea. Presented at the 32nd Midwinter Meeting of the Association for Research in Otolaryngology, Baltimore, February 14–19.

Kim CH, Kim HY, O Chang S, Oh SH, Lee JE, Lee JH (2009b) Developmental change of Na^+-absorptive function in Reissner's membrane epithelia. Neuroreport 20:1275–1278.

Kim SH, Kim KX, Raveendran NN, Wu T, Pondugula SR, Marcus DC (2009) Regulation of ENaC-mediated sodium transport by glucocorticoids in Reissner's membrane epithelium. Am J Physiol Cell Physiol 296:C544–C557.

King M, Housley GD, Raybould NP, Greenwood D, Salih SG (1998) Expression of ATP-gated ion channels by Reissner's membrane epithelial cells. Neuroreport 9:2467–2474.

Kunzelmann K, Bachhuber T, Regeer R, Markovich D, Sun J, Schreiber R (2005) Purinergic inhibition of the epithelial Na^+ transport via hydrolysis of PIP2. FASEB J 19:142–143.

Lazarowski ER, Homolya L, Boucher RC, Harden TK (1997) Direct demonstration of mechanically induced release of cellular UTP and its implication for uridine nucleotide receptor activation. J Biol Chem 272:24348–24354.

Lee JH, Marcus DC (2003) Endolymphatic sodium homeostasis by Reissner's membrane. Neuroscience 119:3–8.

Lee JH, Marcus DC (2008) Purinergic signaling in the inner ear. Hear Res 235:1–7.

Lee JH, Chiba T, Marcus DC (2001) $P2X_2$ receptor mediates stimulation of parasensory cation absorption by cochlear outer sulcus cells and vestibular transitional cells. J Neurosci 21:9168–9174.

Lehrmann H, Thomas J, Kim SJ, Jacobi C, Leipziger J (2002) Luminal P2Y2 receptor-mediated inhibition of Na^+ absorption in isolated perfused mouse CCD. J Am Soc Nephrol 13:10–18.

Leipziger J (2003) Control of epithelial transport via luminal P2 receptors. Am J Physiol Renal Physiol 284:F419–F432.

Loussouarn G, Park KH, Bellocq C, Baró I, Charpentier F, Escande D (2003) Phosphatidylinositol-4,5-bisphosphate, PIP2, controls KCNQ1/KCNE1 voltage-gated potassium channels: a functional homology between voltage-gated and inward rectifier K^+ channels. EMBO J 22:5412–5421.

Ma HP, Chou CF, Wei SP, Eaton DC (2007) Regulation of the epithelial sodium channel by phosphatidylinositides: experiments, implications, and speculations. Pflugers Arch 455:169–180.

Mall M, Wissner A, Gonska T, Calenborn D, Kuehr J, Brandis M, Kunzelmann K (2000) Inhibition of amiloride-sensitive epithelial Na^+ absorption by extracellular nucleotides in human normal and cystic fibrosis airways. Am J Respir Cell Mol Biol 23:755–761.

Marcus DC (1996) Vibrating probes: new technology for investigation of endolymph homeostasis. Keio J Med 45:301–305.

Marcus DC, Chiba T (1999) K^+ and Na^+ absorption by outer sulcus epithelial cells. Hear Res 134:48–56.

Marcus DC, Scofield MA (2001) Apical P2Y4 purinergic receptor controls K^+ secretion by vestibular dark cell epithelium. Am J Physiol Cell Physiol 281:C282–C289.

Marcus DC, Shipley AM (1994) Potassium secretion by vestibular dark cell epithelium demonstrated by vibrating probe. Biophys J 66:1939–1942.

Marcus DC, Sunose H, Liu J, Bennett T, Shen Z, Scofield MA, Ryan AF (1998) Protein kinase C mediates P2U purinergic receptor inhibition of K+ channel in apical membrane of strial marginal cells. Hear Res 115:82–92.

Marcus DC, Liu J, Lee JH, Scherer EQ, Scofield MA, Wangemann P (2005) Apical membrane P2Y4 purinergic receptor controls K^+ secretion by strial marginal cell epithelium. Cell Commun Signal 3:13.

Matos JE, Sorensen MV, Geyti CS, Robaye B, Boeynaems JM, Leipziger J (2007) Distal colonic Na^+ absorption inhibited by luminal $P2Y_2$ receptors. Pflugers Arch 454:977–987.

Mizuta K, Iwasa KH, Tachibana M, Benos DJ, Lim DJ (1995) Amiloride-sensitive Na^+ channel-like immunoreactivity in the luminal membrane of some non-sensory epithelia of the inner ear. Hear Res 88:199–205.

Muñoz DJ, Kendrick IS, Rassam M, Thorne PR (2001) Vesicular storage of adenosine triphosphate in the guinea-pig cochlear lateral wall and concentrations of ATP in the endolymph during sound exposure and hypoxia. Acta Otolaryngol 121:10–15.

Parker MS, Onyenekwu NN, Bobbin RP (2003) Localization of the P2Y4 receptor in the guinea pig organ of Corti. J Am Acad Audiol 14:286–295.

Pochynyuk O, Bugaj V, Vandewalle A, Stockand JD (2008) Purinergic control of apical plasma membrane PI(4,5)P2 levels sets ENaC activity in principal cells. Am J Physiol Renal Physiol 294:F38–F46.

Ralevic V, Burnstock G (1998) Receptors for purines and pyrimidines. Pharmacol Rev 50:413–492.

Robaye B, Boeynaems JM, Communi D (1997) Slow desensitization of the human P2Y6 receptor. Eur J Pharmacol 329:231–236.

Sage CL, Marcus DC (2002) Immunolocalization of P2Y4 and P2Y2 purinergic receptors in strial marginal cells and vestibular dark cells. J Membr Biol 185:103–115.

Stockand JD, Bao HF, Schenck J, Malik B, Middleton P, Schlanger LE, Eaton DC (2000) Differential effects of protein kinase C on the levels of epithelial Na^+ channel subunit proteins. J Biol Chem 275:25760–25765.

Szücs A, Szappanos H, Tóth A, Farkas Z, Panyi G, Csernoch L, Sziklai I (2004) Differential expression of purinergic receptor subtypes in the outer hair cells of the guinea pig. Hear Res 196:2–7.

Tao L, Harris AL (2007) 2-aminoethoxydiphenyl borate directly inhibits channels composed of connexin26 and/or connexin32. Mol Pharmacol 71:570–579.

Thomas J, Deetjen P, Ko WH, Jacobi C, Leipziger J (2001) $P2Y_2$ receptor-mediated inhibition of amiloride-sensitive short circuit current in M-1 mouse cortical collecting duct cells. J Membr Biol 183:115–124.

von Kügelgen I (2006) Pharmacological profiles of cloned mammalian P2Y-receptor subtypes. Pharmacol Ther 110:415–432.

Wangemann P (2002) K^+ cycling and its regulation in the cochlea and the vestibular labyrinth. Audiol Neurootol 7:199–205.

Wildman SS, Unwin RJ, King BF (2003) Extended pharmacological profiles of rat P2Y2 and rat P2Y4 receptors and their sensitivity to extracellular H^+ and Zn^{2+} ions. Br J Pharmacol 140:1177–1186.

Xu SZ, Zeng F, Boulay G, Grimm C, Harteneck C, Beech DJ (2005) Block of TRPC5 channels by 2-aminoethoxydiphenyl borate: a differential, extracellular and voltage-dependent effect. Br J Pharmacol 145:405–414.

Yamamoto T, Suzuki Y (2002) Role of luminal ATP in regulating electrogenic Na^+ absorption in guinea pig distal colon. Am J Physiol Gastrointest Liver Physiol 283:G300–G308.

Yeh TH, Tsai MC, Lee SY, Hsu MM, Tran Ba Huy P (1997) Stretch-activated nonselective cation, Cl^- and K^+ channels in apical membrane of epithelial cells of Reissner's membrane. Hear Res 109:1–10.

Yeh TH, Herman P, Tsai MC, Tran Ba Huy P, Van den Abbeele T (1998) A cationic nonselective stretch-activated channel in the Reissner's membrane of the guinea pig cochlea. Am J Physiol 274:C566–C576.

Zdebik AA, Wangemann P, Jentsch TJ (2009) Potassium ion movement in the inner ear: insights from genetic disease and mouse models. Physiology (Bethesda) 24:307–316.

Zhong SX, Liu ZH (2004) Immunohistochemical localization of the epithelial sodium channel in the rat inner ear. Hear Res 193:1–8.